ADVANCED HEALTHCARE MATERIALS
www.advhealthmat.de

Bioinspired Nanoparticulate Medical Glues for Minimally Invasive Tissue Repair

*Yuhan Lee, Chenjie Xu, Monisha Sebastin, Albert Lee, Nathan Holwell, Calvin Xu, David Miranda Nieves, Luye Mu, Robert S. Langer, Charles P. Lin, and Jeffrey M. Karp**

Delivery of tissue glues through small-bore needles or trocars is critical for sealing holes, affixing medical devices, or attaching tissues together during minimally invasive surgeries. Inspired by the granule-packaged glue delivery system of sandcastle worms, a nanoparticulate formulation of a viscous hydrophobic light-activated adhesive based on poly(glycerol sebacate)-acrylate is developed. Negatively charged alginate is used to stabilize the nanoparticulate surface to significantly reduce its viscosity and to maximize injectability through small-bore needles. The nanoparticulate glues can be concentrated to ≈30 w/v% dispersions in water that remain localized following injection. With the trigger of a positively charged polymer (e.g., protamine), the nanoparticulate glues can quickly assemble into a viscous glue that exhibits rheological, mechanical, and adhesive properties resembling the native poly(glycerol sebacate)-acrylate based glues. This platform should be useful to enable the delivery of viscous glues to augment or replace sutures and staples during minimally invasive procedures.

1. Introduction

Methods to seal tissue leaks, attach devices, and to join tissues together during minimally invasive surgeries represent a significant challenge. Current surgical techniques that include sutures and staples are difficult to perform accurately through a narrow incision do not provide a waterproof seal, and the materials used typically exhibit a mechanical mismatch with tissue and can cause tissue damage.[1–5] Tissue adhesives and sealants used in clinic include fibrin sealants (e.g., Tisseel), cyanoacrylate-based glues (e.g., Histoacryl, Dermabond, Omnex), and protein/peptide-based glues (e.g., BioGlue, TissuGlu), however their use in minimally invasive procedures is limited due to suboptimal usability/controllability by surgeons as they are generally applied in a low viscosity state, are hydrophilic, and can dilute in blood or other fluids, and it is typically difficult to control their adhesive activation. Furthermore, current tissue adhesives often do not exhibit the right level of adhesion in wet surgical fields and some exhibit toxicity for certain applications.[6–11] Polymeric glues have been developed that are promising for use in minimally invasive procedures given their hydrophobic properties to repel tissue fluids at the target site, their viscosity to remain in place following delivery, and their light activated on-demand adhesion.[12] However, the viscosity can present challenges when delivery is required through small-bore needles, especially, during procedures such as endoscopic and laparoscopic surgeries and surgeries on fragile tissues within confined space (e.g., ophthalmic applications). A remaining challenge is to enable surgical adhesives to be delivered through narrow channels via introducer devices (e.g., endoscopes, laparoscopes, or syringe needles) with precise control over the amount and the application site of the surgical glues.[13] To maximize the injectability of glues, dilution using oils (e.g., lipiodol) or inclusion of low molecular weight monomers can be employed to reduce viscosities, yet are non-ideal given that the adhesion properties and amount of time required to activate adhesion are inevitably compromised and such approaches can increase potential toxicity.[14,15] As an alternative method, needle-free injection using jet injectors have been developed to deliver viscous fluids in a transdermal route without inducing skin lesions.[16–19] However, it is challenging

Dr. Y. Lee, Dr. C. Xu, M. Sebastin, A. Lee, N. Holwell, C. Xu, D. Miranda Nieves, L. Mu, Prof. J. M. Karp
Department of Medicine
Center for Regenerative Therapeutics
Brigham and Women's Hospital
Harvard Medical School
Harvard Stem Cell Institute
Harvard-MIT Division of Health Science and Technology
65 Landsdowne Street, Cambridge, MA 02139, USA
E-mail: jmkarp@partners.org
Prof. R. S. Langer
Harvard–Massachusetts Institute of Technology
Division of HealthSciences and Technology
Institute for Medical Engineering & Science
Massachusetts Institute of Technology
David H. Koch Institute for Integrative Cancer Research
Massachusetts Institute of Technology
Department of Chemical Engineering
Massachusetts Institute of Technology
Cambridge, MA 02139, USA
Prof. C. P. Lin
Wellman center for Photomedicine
Massachusetts General Hospital
Harvard Medical School
Boston, MA 02140, USA

DOI: 10.1002/adhm.201500419

to control the injection depth and this approach would be difficult to apply for minimally invasive internal procedures. There is an urgent need to develop approaches to enable the delivery of viscous medical adhesives through small-bore needles or trocars without compromising the adhesion force or safety.

Inspired by the viscous glue secretion mechanism of the sandcastle worm (*Phragmatopoma californica*), we have developed a nanoencapsulated viscous glue that can easily be injected through small-bore needles for application during minimally invasive procedures. Many marine species such as barnacles and marine mussels secrete high concentrations of protein glues into a mixing chamber where precursors are combined and are isolated from the surrounding environment.[20–27] This creates a unique plaque-and-thread structure that immobilizes the animal body to the substrate. By contrast, the sandcastle worms secrete glues into the surrounding environment without clogging their secretory ducts to build a tube-shaped house that makes use of accessible particulates including sand particles.[28–31] To achieve this, high concentrations of proteinaceous glues are packaged into micrometer-sized granules and stored in secretory cells (**Figure 1**a). When they are signaled to release the glues via a "burst" response, these granules are quickly delivered through secretory ducts into seawater that contains rich electrolytes and high pH (>8.0). The electrolytes in seawater trigger the granule membranes to rupture to release their glue contents resulting in viscous bulk glue mass that further cures to bond surrounding objects (e.g., sand particles). Inspired by the granule-based controlled glue transportation/activation system of sandcastle worms, we demonstrate a strategy to formulate viscous glues into water-dispersible injectable glue nanoparticles that can be assembled into the native viscous glue state following injection and can be cured in response to on-demand external stimuli (Figure 1b). As a model viscous water-insoluble glue, we used hydrophobic light-activating adhesive (HLAA).[12] HLAA is a polymeric UV-activated adhesive based on water-insoluble poly(glycerol sebacate)-acrylate (PGSA) polymer. Previously we showed that the glue could be delivered on a patch to a challenging target site (e.g., inside a beating heart) without washout where blood generates significant shear stress. HLAA is a viscous polymer system having viscosity more than 50 mPa s that is generally regarded as the maximum viscosity of any liquid to be injectable through 27-gauge hypodermic needle (nominal inner diameter: 0.21 mm), although this requires significant force. To develop an injectable formulation of HLAA, we coated viscous HLAA nanoparticles with a negatively charged water-soluble alginate that served to temporarily detackify the glue precursor (average diameter: 250–500 nm). The injectability of the nanoparticle dispersions was studied and the reformulation of the nanoparticles into the native HLAA with a positive-charged polymer trigger was also investigated. To demonstrate the use of the nanoparticle glues in ophthalmic applications where surgical access is highly limited, intravitreal injection of the nanoparticle glue was evaluated for the potential application in retina repair.

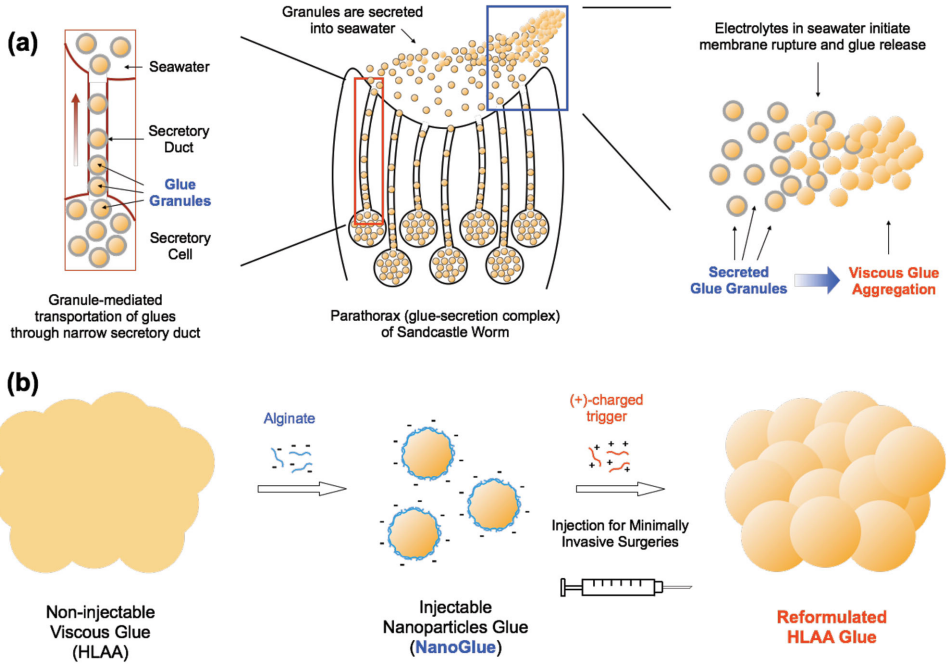

Figure 1. Schematic representation of nanoparticulate glues (NanoGlue) inspired by the granule-mediated glue transportation system of sandcastle worms. a) Sandcastle worms condense high concentration proteinaceous glues into micrometer-sized granules to secret viscous glues through narrow secretory ducts. When the granules are secreted and exposed to the electrolyte-rich seawater, their membrane ruptures to release viscous glues. The glues aggregate into a bulk mass that further cures to attach surrounding objects. b) Schematic representation of fabrication of the bioinspired injectable NanoGlue nanoparticles using alginate as a surfactant to encapsulate the hydrophobic viscous glue HLAA. When they are exposed to positive-charged trigger molecules, NanoGlue particles aggregate to form a viscous glue that is similar to the native HLAA.

Adv. Healthcare Mater. **2015**,
DOI: 10.1002/adhm.201500419

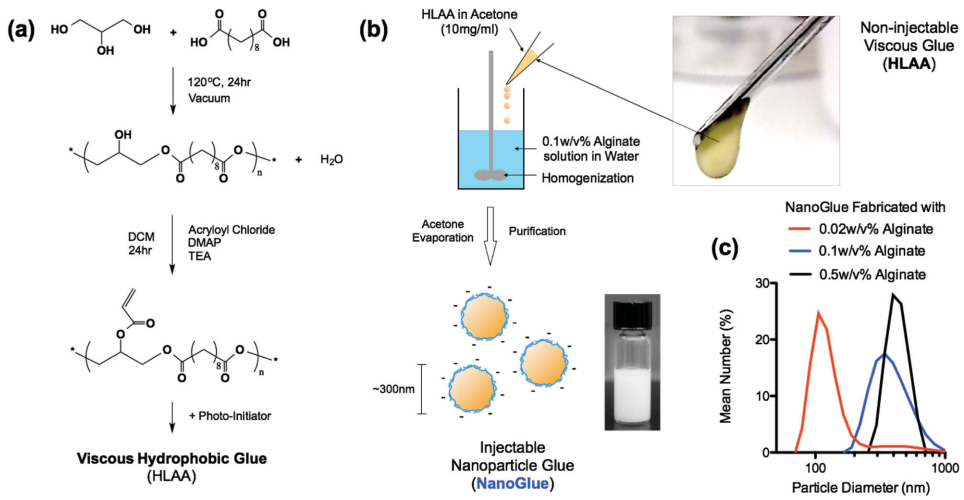

Figure 2. Synthesis of the hydrophobic viscous glue HLAA and fabrication of NanoGlue particles. a) Synthesis scheme of the hydrophobic viscous glue HLAA. Glycerol and sebacic acid were polymerized using polycondensation reaction and further conjugated with acrylate groups to fabricate UV cross-linkable glue. Degree of acrylation was 0.5 mol per 1 mol of hydroxyl groups in the polymer backbone. b) Fabrication of NanoGlue nanoparticles using single-emulsion method. The viscous HLAA was dissolved in acetone (10 mg mL^{-1}) and added in 0.1 w/v% sodium alginate solution (pH adjusted to 7.0) with homogenization. After evaporation of acetone and purification using centrifugation/resuspension cycles, the white turbid NanoGlue particle dispersions were formulated. c) Size distribution of NanoGlue particles in aqueous solutions measured using dynamic light scattering (DLS). The NanoGlue particles were fabricated in sodium alginate solutions with three different concentrations (0.02, 0.1, and 0.5 w/v%). The NanoGlue particles had average sizes of 150.8 ± 54.6 nm, 267.7 ± 36.9 nm, and 408.2 ± 25.1 nm when fabricated in 0.02 w/v% (red bars), 0.1 w/v% (blue bars), and 0.5 w/v% (black bars) aqueous sodium alginate solutions, respectively. Due to the instability of NanoGlue particles fabricated with sodium alginate concentration less than 0.1 w/v%, the NanoGlue particles fabricated in 0.1 w/v% sodium alginate solution was used in all the further studies.

2. Results and Discussion

2.1. Fabrication of Stable HLAA Nanoparticles and Injectability

We envisioned that the ideal injectable nanoparticle HLAA (NanoGlue) should (1) have low resistance during injection through a small-bore needle, (2) be rapidly injectable within seconds, (3) not clog the needle during placement or injection, (4) be capable of rapid transition into a continuous mass after injection, (5) exhibit on demand curing as a single mass, and (6) achieves the adhesion force of the native glue. To fabricate the viscous hydrophobic glue HLAA, PGSA (degree of acrylation: 0.5) was synthesized by acrylation of low molecular weight poly(glycerol sebacate) (PGS, weight average molecular weight: 5.0 ± 0.4 kDa) followed by the addition of a water-insoluble photoinitiator (0.2 w/v% in HLAA) to avoid wash out in water (**Figure 2**a). In our previous study, the HLAA glue showed minimal inflammation and necrosis in animal models indicating the biocompatibility of the glue.[12] In a typical surgical scenario with HLAA, the viscous glue was placed manually (e.g., via a spatula). To transform the hydrophobic viscous liquid into nontacky stable nanoparticles, negatively charged low viscosity alginate was selected as a candidate particle surface stabilizer (Figure 2b) based on its well-established biocompatibility. When the alginate molecules bind to the surface of the HLAA nanoparticles (potentially via physical adsorption), it was expected to lower the surface tension of the liquid to prevent them from rapid aggregation and phase separation. In addition, when the alginate-coated nanoparticles are exposed to oppositely charged substances, the highly negative surface charge from alginate promotes efficient agglomeration/transition from nanoparticles to bulk glue. To fabricate the HLAA nanoparticles coated with alginate (NanoGlue), HLAA (100 mg) was dissolved in acetone (10 mL) and added into an alginate solution in water (20 mL, pH 7.0) drop wise with homogenization for 5 min followed by overnight evaporation of acetone and three centrifuge/dispersion cycles for purification. The resultant NanoGlue particles had average particle sizes of 267.7 ± 36.9 nm (fabricated in 0.1 w/v% sodium alginate) and 408.2 ± 25.1 nm (fabricated in 0.5 w/v% sodium alginate) measured by dynamic light scattering (DLS). The NanoGlue nanoparticles fabricated with the sodium alginate concentration higher than 0.1 w/v% could be dispersed in distilled water or phosphate buffered saline (PBS) (pH 7.4) and remain stable at 4 °C for at least two weeks without any noticeable change in the average size measured by DLS. The NanoGlue particles fabricated with 0.02 w/v% sodium alginate initially formed nanoparticles with the diameter of 150.8 ± 54.6 nm, but quickly formed a viscous aggregation on the bottom of a container within 3 d suggesting that there was an insufficient amount of alginate emulsifier on the surface of the NanoGlue. The zeta potentials of the NanoGlues fabricated with 0.02, 0.1, and 0.5 w/v% sodium alginate were −11.8 ± 2.4 mV, −50.0 ± 4.0 mV, and −48.8 ± 5.3 mV, respectively, indicating that the alginate coating is saturated at 0.1 w/v%. This is also consistent with improved stability of the NanoGlue particles with 0.1 and 0.5 w/v% alginate compared to the particles fabricated with lower 0.02 w/v% alginate. Therefore, NanoGlue particles fabricated with 0.1 w/v% sodium alginate solution were used in all the further studies.

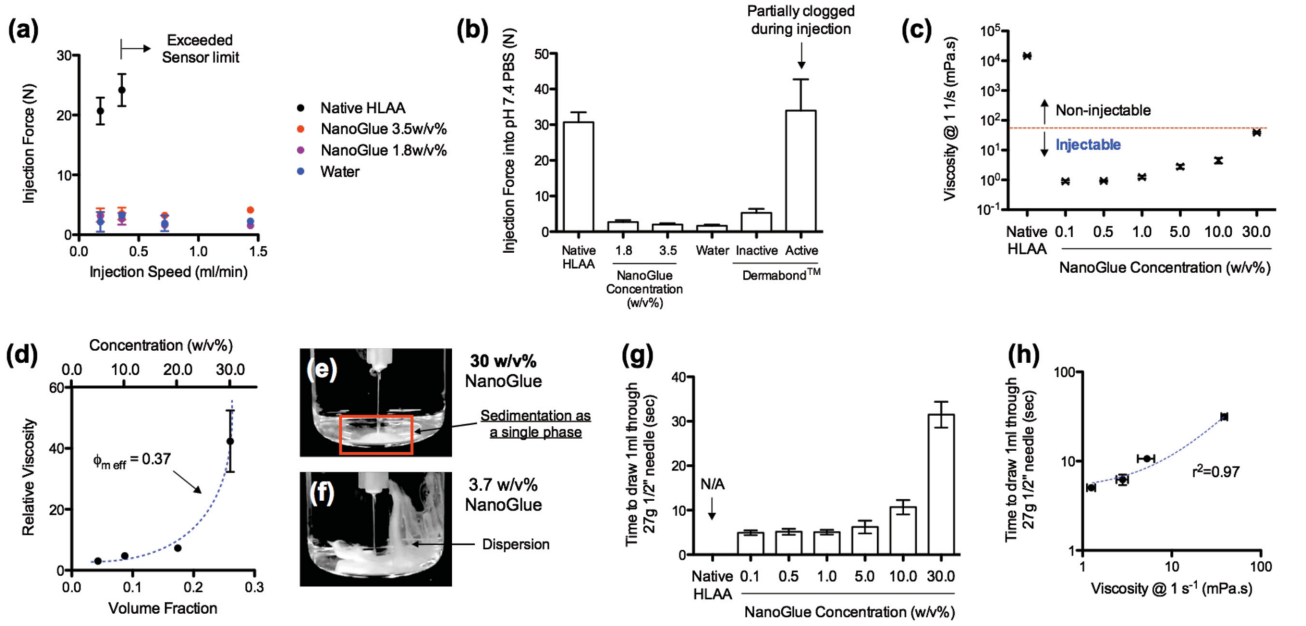

Figure 3. NanoGlue particle dispersions at concentrations up to 30 w/v% in water are injectable through 27-gauge 1/2 in. needles. a) Injection forces of native HLAA (black dots), 3.5 w/v% NanoGlue dispersions (red dots), 1.8 w/v% NanoGlue dispersions (purple dots), and water (blue dots) at injection speeds from 0.18 to 1.44 mL min^{-1}. The liquids were injected vertically into air. The injection force could not be measured with native HLAA at speeds over 0.36 mL min^{-1} because it exceeded the detection limit of the force sensor (≈50 N). b) Injection forces of native HLAA, NanoGlue dispersions (3.5 and 1.8 w/v% in water), water, and Dermabond into pH 7.4 PBS. The injection speed was 0.36 mL min^{-1}. Activated form of Dermabond partially clogged the tip of the needle during injection into PBS. c) Viscosity of native HLAA and NanoGlue particle dispersions (0.1–30.0 w/v% in water). The viscosity of ≈50 mPa s is generally considered as injectable (red dashed line).[44,45] d) Correlation between experimental volume ratios and relative viscosity of NanoGlue particle dispersions. Concentration of each sample is indicated in upper *x*-axis. The plot was fitted in the semiempirical model of Krieger and Dougherty that predicts the viscosity change of nanoparticle dispersions at different concentrations: $\eta_r = (1 - \phi/\phi_{m\,eff})^{-2}$, where η_r is the relative viscosity, ϕ is the volume fraction, and $\phi_{m\,eff}$ is the effective maximum packing fraction. The $\phi_{m\,eff}$ was 0.37 ($r^2 = 0.89$) indicating that the viscosity of NanoGlue dispersions would increase more drastically in volume fractions (i.e., volumetric concentrations) close to 0.37 (42.6 w/v% of NanoGlue dispersion). This was in good agreement with the maximum injectable concentration of ≈30 w/v% in Figure 3c. e) Representative image of 30 w/v% NanoGlue dispersions injected into pH 7.4 PBS. The NanoGlue dispersions were flocculated on the bottom of the vial as a separate phase liquid (i.e., without dispersion) (see also Movie S1, Supporting Information) indicating that the 30 w/v% NanoGlue dispersions would not easily diffuse into the surrounding environment. f) Representative image of 3.7 w/v% NanoGlue dispersions injected into pH 7.4 PBS. The NanoGlue dispersions were slowly dispersed into PBS (see also Movie S2, Supporting Information). g) Time to draw 1 mL of native HLAA and NanoGlue dispersions (0.1–30.0 w/v%) through 27-gauge 1/2 in. needles. HLAA was unable to draw through the narrow needles. h) Correlation between viscosity and time to draw 1 mL of NanoGlue dispersions in different concentrations (0.1–30.0 w/v%) through 27-gauge 1/2 in. needles. To obtain the correlation coefficient (i.e., r^2), the plot was fitted to Hagen–Poiseuille equation (blue dashed line): $\Delta P = 8\mu LQ/\pi r^4$, where ΔP is the pressure loss, L is the length of the needle, μ is the dynamic viscosity of the fluid, Q is the volumetric flow rate, and r is the radius of the needle.

To evaluate the force that the surgeons would experience to inject NanoGlue particle dispersions through a narrow needle, we loaded HLAA or NanoGlue dispersions (1.8 and 3.5 w/v%) into a 1 mL syringe attached with a 27-gauge 1/2 in. syringe (inner diameter: 0.210 mm, length: 0.5 in), and measured the force required to achieve a predetermined flow rate (0.18, 0.36, 0.72, and 1.44 mL min^{-1}) during the injection (**Figure 3**a). When the native HLAA was injected, high resistance was observed in low injection velocity, and in higher injection velocities above 0.36 mL min^{-1} the force exceeded the technical limit of the force sensor (>50 N). Considering that the typical hypodermic injection technique takes less than a minute to inject 1 mL of water using 27-gauge needles, the HLAA can be regarded as noninjectable through 27-gauge needles. By contrast, when the syringe was loaded with the 1.8 or 3.5 w/v% NanoGlue dispersions, there was low resistance at higher injection speed of 0.72 and 1.44 mL min^{-1}. The forces required to inject the NanoGlue dispersions at the rate of 0.72 mL min^{-1} were 1.63 ± 0.16 N for 1.8 w/v% dispersions and 3.23 ± 0.19 N for 3.5 w/v% dispersion that were significantly lower than the native HLAA (exceeded sensor limit of 50 N) and were similar to the injection force of water (1.83 ± 1.08 N). In minimally invasive procedures such as intraocular glue injection for retina repair and endoscopic surgeries using narrow bore injection devices, injection of glues into aqueous environment is desired (e.g., vitreous, stomach wall) without clogging the needle.[32,33] When the NanoGlue dispersions were injected into pH 7.4 PBS buffer (injection speed: 0.36 mL min^{-1}, Figure 3b), the injection forces (2.70 ± 0.52 N for 3.5 w/v% NanoGlue and 1.96 ± 0.41 N for 1.8 w/v% NanoGlue) were similar to the forces required to inject water into pH 7.4 PBS (1.64 ± 0.36 N) and also similar to the forces when they were injected into open air as shown in Figure 3a. However, cyanoacrylates, one of the primary adhesives considered in clinical practice that require injection through narrow channels (e.g., gastric varices treatment, ophthalmic surgeries),[10,15,33–35] can be nonspecifically activated when they are exposed to an

Adv. Healthcare Mater. **2015**,
DOI: 10.1002/adhm.201500419

aqueous environment and potentially clog the tip of the needles or endoscopic channels (e.g., gastric varices repair).[33,36] When Dermabond in its inactive form was injected into pH 7.4 PBS, the injection force was moderately higher than the force to inject water or NanoGlue dispersions (5.27 ± 1.11 N). When the activator was added to Dermabond as recommended by manufacturer and injected using the same method, it quickly formed a stiff glue residue at the tip of the needle during injection (Figure 3c) and the injection force was rapidly increased up to 33.94 ± 8.80 N.

To maximize the concentration of the NanoGlue for rapid transformation upon exposure with positive charged substance, the correlation between NanoGlue concentration and injectability was investigated. A semiempirical model of Krieger and Dougherty describes that particle crowding enhances hydrodynamic interactions between particles, resulting in significant increase in viscosity with a relatively small increment of particle concentration: $\eta_r = (1 - \varphi/\varphi_{m\ eff})^{-2}$, where η_r is the relative viscosity, φ is the volume fraction, and $\varphi_{m\ eff}$ is the effective maximum packing fraction.[37,38] Therefore, when NanoGlue concentration is increased, it is expected that the viscosity would steeply increase, and the NanoGlue dispersion would behave like a single-phase liquid as the interaction between particles increases. First, to develop the correlation between the NanoGlue particle concentration and the viscosity, dynamic viscosities of NanoGlue dispersions with different concentrations (0.1–30 w/v%) were measured using a rheometer. The viscosity of NanoGlue steeply increased as a function of concentration up to 38.9 ± 3.0 mPa s in 30 w/v% (the maximum concentration that the NanoGlue dispersion could reach 38.5 w/v%) (Figure 3c), and the correlation was well fitted to the Krieger and Dougherty model with the maximum packing fraction $\phi_{m\ eff}$ = 0.37 (r^2 = 0.89) (Figure 3d). Considering that 50 mPa s is usually considered as the upper limit of injection using 25- to 27-gauge needles (red dashed line in Figure 3c), the 30 w/v% NanoGlue dispersion is in the injectable viscosity range. To demonstrate the behavior of NanoGlue dispersions in aqueous solutions, the NanoGlue dispersions with high particle concentration (30 w/v%) close to maximum packing density and low particle concentration (3.7 w/v%) were injected into pH 7.4 PBS. The high concentration NanoGlue dispersion flocculated as a separate phase in PBS (Figure 3e and Movie S1, Supporting Information) due to the substantial interaction between the particles, but when in low concentration, the particles dispersed into PBS (Figure 3f and Movie S2, Supporting Information). This single-phase behavior was observed only near the effective maximum packing fraction (i.e., 30 w/v%) where the particle-to-particle interaction is the highest. This single-phase behavior of the high concentration NanoGlue dispersion is beneficial for medical applications (e.g., intraocular injection targeting the retina surface) because the dispersion could remain at the injection site before activation without dilution even on tissues submersed in water (e.g., vitreous), thus maximizing the interaction with tissue when it is cured.

To further assess the injectability of the high concentration dispersions with increased viscosity, the time required to draw 1 mL of NanoGlue dispersions with different concentrations (0.1–30 w/v%) using 27-gauge 1/2 in. hypodermic needles was measured. In each experiment, the tip of the needle attached on a 1 mL syringe was dipped into the dispersion vertically and the plunger was quickly pulled up to 1 mL and the time required to draw 1 mL was measured. NanoGlue dispersions could be easily drawn in ≈10 s for 10 w/v% NanoGlue dispersions (Figure 3g). The 1 mL 30 w/v% NanoGlue dispersion could be fully drawn in 31.5 ± 2.9 s. Considering glues are usually applied as a thin layer and the amount required to achieve adhesion is minimal (e.g., a few drops of glue dispersion with total volume of less than 0.1 mL are required for ophthalmic applications),[10,39,40] it takes only a few seconds to apply 30 w/v% NanoGlue dispersions to a target site. The native HLAA glue could not be drawn through the 27-gauge 1/2 in. needles. Hagen–Poiseuille equation predicts the hydraulic flow behavior of viscous liquids generated from the pressure difference between each side of a narrow channel.[41–43] In the equation, viscosity is inversely correlated to the volumetric flow rate of the liquid: $\Delta P = 8\mu LQ/\pi r^4$, where ΔP is the pressure loss, L is the length of the needle, μ is the dynamic viscosity of the fluid, Q is the volumetric flow rate, and r is the radius of the needle. If we convert the volumetric flow rate Q (volume/time) to the time required to flow a fixed amount of liquid, the flow rate of NanoGlue can be fitted using the equation (r^2 = 0.97) (Figure 3h) suggesting that the NanoGlue dispersions develop stable laminar (i.e., not turbulent) flow during injection and the velocity is lower than the maximum threshold to generate turbulent flow (see also Figure 3e,f and Movies S1 and S2, Supporting Information).

2.2. Reformulation of NanoGlue Particles into Viscous Glues with Similar Properties to Native HLAA through Addition of Positively Charged Agents

In sandcastle worm glue granules, the surface charge of the granules across the granular membrane plays an important role in the membrane rupture and release of the glues from the granules. When sandcastle worms secrete glue granules into seawater, the high electrolyte concentration and high pH (>8) rapidly destabilizes the granule surface charge that was originally induced from the imbalanced equilibrium of charged substance across the membrane (i.e., Donnan equilibrium). This destabilization further initiates the membrane rupture to release the encapsulated glue components (e.g., mucin, Pc4, Pc3A,B) that rapidly coalesce into a continuous paste-like mass. We aimed to employ the external electrolyte-initiated granular surface destabilization scheme of sandcastle worms to trigger the coalescence of NanoGlue particles by adding oppositely charged electrolytes. It was anticipated that for the NanoGlue particles the oppositely charged electrolytes (e.g., positively charged polymers) could neutralize the surface charge of the NanoGlue particles to initiate the coalescence. We chose protamine, a naturally derived arginine-rich protein (and has been used clinically to neutralize heparin with maximum dose of 50 mg per injection at a concentration of 10 mg mL^{-1} in 0.9 w/v% normal saline) as a trigger for the NanoGlue coalescence process. To visualize the conversion from NanoGlue particles to bulk HLAA mass, fluorescence-labeled alginate (alginate-rhodamine) was used to fabricate fluorescent NanoGlue. Diluted fluorescence-tagged NanoGlue dispersion at a concentration of 1.8 wt% was placed on a glass slide and combined with a

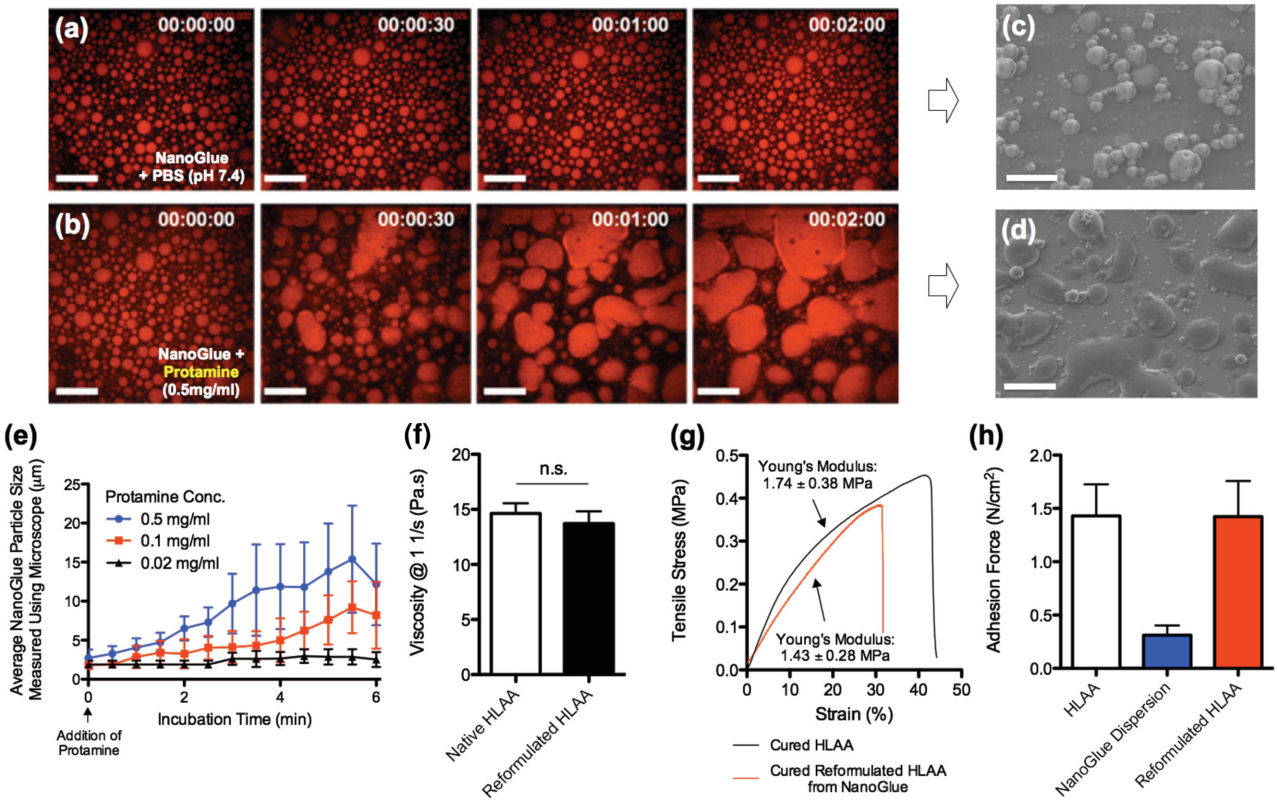

Figure 4. Assembly of NanoGlue particles with protamine into viscous glues exhibits similar properties to native HLAA. a,b) Representative confocal fluorescent images of fluorescent NanoGlue particles on glass slides treated with a) pH 7.4 PBS, or b) 0.5 mg mL^{-1} protamine solution in PBS (pH 7.4). The images were taken in 0, 30, 60, and 120 s after each solution was added. All scale bars indicate 5 μm. c,d) Scanning electron microscopy (SEM) images of NanoGlue particles treated with c) pH 7.4 PBS, or d) 0.5 mg mL^{-1} protamine solution in PBS (pH 7.4). The scale bars indicate 10 μm. e) Change of NanoGlue particle size treated with protamine solutions (0.02, 0.1, and 0.5 mg mL^{-1}). Average particle sizes were measured from images obtained using confocal microscopy. f) Viscosity of native HLAA (white bar) and reformulated HLAA from NanoGlue particles (black bar). g) Representative tensile stress–strain curves of cured HLAA (black line) and cured reformulated HLAA from NanoGlue particles (red line). The glues were cured under UV (0.38 W cm^{-2} at 365 nm wavelength for 10 s) in the thickness of 1.0 mm and cut in dog bone shape for tensile tests. h) Adhesion forces of native HLAA (white bar), 30 w/v% NanoGlue dispersions in water (blue bar), and reformulated HLAA from NanoGlue particles (red bar) on epicardium (heart) tissue.

protamine solution in water (0.5 mg mL^{-1}). When the NanoGlue particles were added with water, the particles retain their size and shape without coalescence even though the particles constantly collided each other (**Figure 4**a and Movie S3, Supporting Information) indicating that the surface charge from the alginate formed repulsive barriers around the NanoGlue particles. In contrast, as shown in Figure 4b and Movie S4 (Supporting Information), the addition of protamine induced the rapid coalescence of NanoGlue particles into microsized bulky masses (5–30 μm) indicating the repulsive barriers from alginate were neutralized to transform the particle surface more attractive to other particles. Scanning electron microscopy (SEM) images of the NanoGlue particles and the NanoGlue particles added with protamine also showed that the charge neutralization by protamine could also trigger stickiness of the particles to a given substrate. The particles without protamine maintain the spherical shape and high contact angle on a hydroxylated silicon wafer (Figure 4c), while the coalesced NanoGlue by addition of protamine spread with much lower contact angle (Figure 4d) indicating that protamine can trigger attraction (i.e., stickiness) of the NanoGlue to the hydroxylated silicon substrate. Within 2 min following the addition of 0.5 mg mL^{-1} protamine solution, the average size of aggregates in the images was 15.4 ± 6.2 μm (blue curve in Figure 4e). When lower concentration protamine solutions (0.1 and 0.02 mg mL^{-1}) were added into quiescent NanoGlue particles, the transitions were slower and the final aggregation sizes were smaller indicating that the transition rate depends on the protamine concentration. When higher concentration (30 w/v%) NanoGlue dispersion (0.1 mL) was added with 10 mg mL^{-1} protamine solution (0.1 mL), the originally turbid NanoGlue dispersion was cleared up in less than 5 s forming a sticky and viscous mass that is phase-separated with aqueous dispersion similar to the original hydrophobic HLAA glue. The viscosity of the reformulated HLAA (14.6 ± 0.9 Pa s) was also closely similar to the native HLAA (13.7 ± 1.1 Pa s) (Figure 4f).

To further assess the curing properties of the reformulated HLAA, the reformulated glue was cured with UV exposure and the tensile strengths were measured using mechanical tester. The cured product of reformulated HLAA showed similar

strain–stress curves to the cured native HLAA (Figure 4g). The average Young's moduli were 1.74 ± 0.38 MPa and 1.43 ± 0.28 MPa for native HLAA and reformulated HLAA, respectively. The maximum strain at breaking was slightly lower for reformulated HLAA (42.3% ± 3.3%) compared to the native HLAA (32.8% ± 3.1%). It seems that during the transition of NanoGlue particles into bulk viscous glue, trace amount of aqueous solution became entrapped in the glue in the form of small droplets that generate nanopores upon curing. To compare the adhesion properties of the reformulated HLAA and the native HLAA on a wet tissue, each glue was placed on a UV-transparent and elastic poly(glycerol sebacate)-urethane (PGSU) patch and cured on a heart (epicardium) tissue for pull-off adhesion tests using mechanical tester. The adhesion force of reformulated HLAA on epicardium tissue (1.43 ± 0.30 N cm^{-2}) was closely similar to the native HLAA (1.42 ± 0.34 N cm^{-2}) (Figure 4h). In our previous study, the in vivo adhesion force of the native HLAA was sufficient to successfully close vascular defects and to attach an elastic patch inside a beating pig heart.[12] In the in vivo rat cardiac defect models, the native HLAA successfully sealed the defect for up to six months with minimal short-term and long-term inflammation. We also found that the adhesion force of HLAA was several fold higher than conventional tissue glues including fibrin glues (e.g., TisuSeal) and cyanoacrylate glues (e.g., Dermabond) applied in aqueous environments. Fourier transform-infrared (FT-IR) spectroscopy data (Figure S1, Supporting Information) also showed that there is no apparent difference in chemical structure between the native HLAA and the reformulated HLAA from NanoGlue particles.

2.3. Injection of NanoGlue Particle Dispersions into Biological Tissues and In Situ Rapid Transition into Sticky Glue for Potential Medical Applications

To demonstrate the potential use of NanoGlue system in medical applications, we first hypothesized that, when NanoGlue particles are injected into a porous tissue and immediately triggered to aggregate in situ, they could form bulk sticky masses that would not easily diffuse away from the injection site. To examine this hypothesis, low concentration NanoGlue dispersions (3.7 wt% in water) that are prone to diffusion (see Figure 3f) were subcutaneously injected into mouse ears along with protamine (0.5 mg mL^{-1} in pH 7.4 PBS) or pH 7.4 PBS (**Figure 5**a). To maximize the particle-to-glue conversion rate, a double barrel syringe that intermix the contents from each barrel in an extended mixing channel was used and a 27-gauge 1/2 in. needle was fitted at the tip of the syringe (Figure 5b). Using a custom-built video-rate laser-scanning confocal microscope, the NanoGlue particles were visualized at the injection site 5 min after injection. When NanoGlue particles and PBS (pH 7.4) were co-delivered, NanoGlue particles migrated several hundred micrometers from the injection site (Figure 5c). When NanoGlue particles were co-injected with protamine solution (0.5 mg mL^{-1}), the particles rapidly formed bulk masses with sizes of ≈30–100 µm adjacent to the injection site (Figure 5d) indicating the NanoGlue particles were reformulated into sticky HLAA and remained localized at the injection site for 5 min.

We further aimed to use the NanoGlue system in minimally invasive ophthalmic surgeries such as retina repair for proliferative viteroretinopathy (PVR) where intraocular glue injection

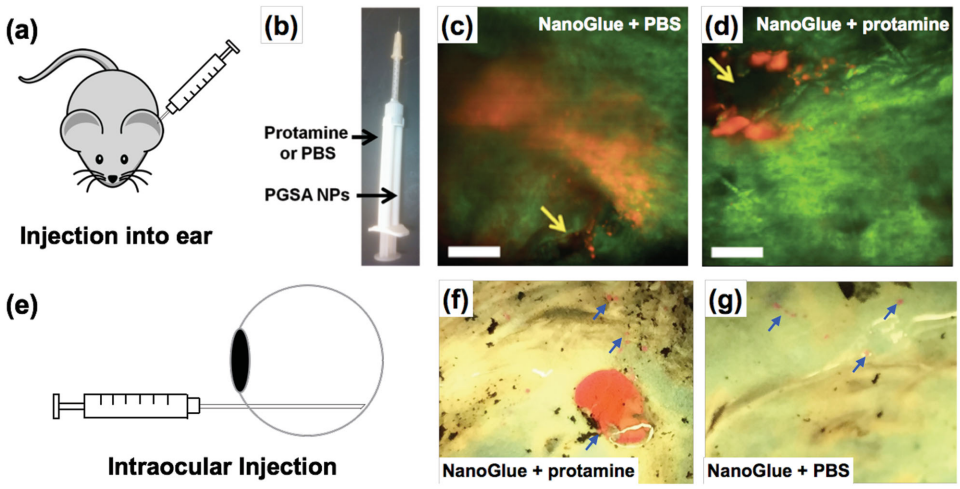

Figure 5. Injection of NanoGlue particle dispersions into biological tissues and in situ rapid transition into a viscous glue for potential medical applications. a–d) To demonstrate the ability of the NanoGlue to reformulate in vivo, NanoGlue particles were injected into an ear of a balb/c mouse and immediately triggered for coalescence in situ. To inject NanoGlue particles, a double-barrel syringe equipped with a mixer and 27-gauge 1/2 in. needle (b) was used. c–d) A custom-built video-rate laser-scanning confocal microscope was used to image the particle distribution of c) NanoGlue particles injected with PBS and d) 3.7 w/v% NanoGlue particles injected with 0.5 mg mL^{-1} protamine solution in 5 min after injections. The alginate on NanoGlue particles was labeled with rhodamine (red in the images in (c,d)). Green fluorescence is generated via the autofluorescence of mouse ear skin under an excitation of 480 nm. Yellow arrows indicate the injection sites. e–g) Potential applications of NanoGlue system in minimally invasive ophthalmic surgeries such as retina repair for proliferative viteroretinopathy (PVR) where intraocular glue injection through a narrow entry is required. Representative images of 30 w/v% NanoGlue dispersions injected with f) 10 mg mL^{-1} protamine solution in PBS (pH 7.4), or g) pH 7.4 PBS. The eyes were dissected in 5 min after injections. To visualize the NanoGlue particles and the reformulated HLAA, the PGSA polymer was labeled using rhodamine-isocyanate resulting in a visible red color under ambient light.

through a narrow entry is required. PVR is a disease that develops as a complication of rhegmatogenous retinal detachment. PVR occurs in about 8%–10% of patients undergoing primary retinal detachment surgery and prevents the successful surgical repair of rhegmatogenous retinal detachment. PVR can be treated with surgery to reattach the detached retina but the visual outcome of the surgery is very poor. Especially, current treatment options insert intraocular tamponade materials (e.g., silicone oils or long-acting gases) in vitreous near the diseased site to press the detached retina onto the retinal pigment epithelium (RPE). However, they are strongly associated with severe complications (e.g., cataracts, glaucoma) and the patient compliance is sub-optimal given that the treatment requires a head-down position for weeks. To address this, recent studies have examined the utility of medical adhesives, however currently available tissue adhesives are potentially toxic (e.g., cyanoacrylate), exhibit low adhesion, or require long times to cure (e.g., fibrin glues) which can lead to rapid diffusion of the glue into the surrounding vitreous.[34] Therefore, we envisioned the NanoGlue system could be useful as an intraocular injectable glue, given that is 1) injectable through a small-bore needle (i.e., 27-gauge needles), 2) not easily washed away after particle aggregation, 3) able to attach strongly in wet environments, and 4) biocompatible. We hypothesized that NanoGlue particle dispersions could be injected into the subretinal region via an intraocular route and then quickly form the sticky and viscous reformulated HLAA. To visualize the NanoGlue particles and the reformulated HLAA, the base polymer PGSA was labeled using rhodamine-isocyanate resulting in visible red color under ambient light. The high concentration red NanoGlue particle dispersion (30 w/v% in water) was drawn into a 1 mL syringe with a 27-gauge 1 in. needle, and the needle was inserted through the anterior part of sclera of a freshly harvested bovine eye. The needle was further maneuvered vertically until it reached the retinal side of the posterior eye, and ≈0.1 mL of the NanoGlue dispersion was injected. The 1 mL syringe was then rapidly replaced with another 1 mL syringe containing 10 mg mL^{-1} protamine solution in distilled water or PBS (pH 7.4), and ≈0.05 mL of the protamine solution (or PBS) was injected onto the same site (total amount of protamine: 0.5 mg). The eyes were dissected 5 min following injection. When NanoGlue dispersion was injected followed by protamine solution, a red-colored mass of the reformulated HLAA was observed isolated on the tapetum lucidum that is located immediately behind the retina (Figure 5e). This may serve useful to reattach the retina on the posterior membrane of the eye. 5 min after injection, the NanoGlue particles delivered with PBS (pH 7.4) either migrated into the vitreous (when delivered without protamine) or were found as a few small masses (with protamine delivery) on the tapetum lucidum (Figure 5f) suggesting that the protamine trigger is critical to prevent dilution of even high concentration NanoGlue dispersions (30 w/v%).

3. Conclusion

In conclusion, we demonstrated a nanoparticulate formulation of a viscous hydrophobic light-activated adhesive (NanoGlue) inspired by the granule-packaged glue delivery system of sandcastle worms. Negatively charged alginate was used to stabilize the NanoGlue surface to significantly reduce its viscosity and to maximize injectability through small-bore needles (i.e., 27-gauge hypodermic needles). The nanoparticulate glues could be concentrated to ≈30 w/v% dispersions in water that remained localized following injection. With the trigger of a positively charged polymer (e.g., protamine), the nanoparticulate glues could quickly coalesce into a viscous glue that exhibits rheological, mechanical, and adhesive properties resembling the native poly(glycerol sebacate)-acrylate based glues. The nanoparticulate glues could be injected into model biological tissues through 27-gauge needles and formed viscous glues on the site of injection with the protamine trigger. This platform should be useful to enable the delivery of viscous glues to augment or replace sutures and staples during minimally invasive procedures.

4. Experimental Section

Synthesis of HLAA: PGS prepolymer was synthesized using the polycondensation reaction between glycerol and sebacic acid. Briefly, 4.6 g of glycerol and 10.3 g of sebacic acid (equimolar amount) were added into a round-bottom flask and reacted in 120 °C for 8 h in nitrogen environment and for 16 h in vacuum (≈50 mm Hg). The resultant PGS prepolymer had molecular weight of 5.0 ± 0.4 kDa, determined using gel permeation chromatography (Viscotek TDA 305 with Agilent 1260 pump and autosampler, Malvern Instruments). The PGS prepolymer was further conjugated with an acrylate moiety using acryloyl chloride. Briefly, 5 g of PGS prepolymer and 5 mg of 4-(dimethylamino)-pyridine (DMAP, 0.0445 mmol) was dissolved in 200 mL of anhydrous dichloromethane. Acryloyl chloride (0.5 mol mol^{-1} glycerol on PGS) and triethylamine (equimolar to acryloyl chloride) were added dropwise for 30 min in an ice bath and reaction was kept for 24 h in room temperature under a nitrogen environment with vigorous stirring. The resultant PGSA was purified using precipitation into ethyl acetate. HLAA was fabricated by adding 0.2 w/v% photoinitiator Irgacure 2959 (BASF) into PGSA. To make fluorescent HLAA, rhodamine-isocyanate was added (0.01 mol mol^{-1} glycerol on PGSA) and reacted overnight. Rhodamine-labeled PGSA was purified using precipitation into ethyl acetate and further added with 0.2 w/v% photoinitiator Irgacure 2959 to prepare fluorescent HLAA.

Fabrication of NanoGlue Particles Using a Single Emulsion and Characterization of the Morphology and Viscosity: NanoGlue particles were prepared using single oil-in-water emulsion method using water and acetone. Briefly, 20 mL of 0.02, 0.1, or 0.5 w/v% sodium alginate (low viscosity, Sigma-Aldrich) solution in water (final pH adjusted to 7.0) was placed in a 50 mL beaker and 10 mL of 1% HLAA solution in acetone was added drop wise for 5 min with homogenization (Tissue Master 125). To fabricate fluorescent NanoGlue particles using fluorescent alginate, 0.1 w/v% sodium alginate conjugated with rhodamine (50 kDa, Creative PEGWorks) was used instead of sodium alginate. The resultant white suspension was further stirred (400 rpm) overnight in the dark to evaporate acetone. The product was centrifuged at 14 000 rpm for 10 min and redispersed in water for three times to separate NanoGlue from the residual alginate, unencapsulated HLAA, and acetone. The hydrodynamic diameter and polydispersity of NanoGlue particles were measured using dynamic light scattering (Malvern Zetasizer Nano ZS90) in water. The product yield was 78% calculated using lyophilized NanoGlue compared to the original HLAA input. To determine the maximum concentration of NanoGlue particles that can remain in suspension the purified NanoGlue suspension was centrifuged at 14 000 rpm for 10 min and the supernatant was carefully removed and the weight was measured. The concentrated NanoGlue dispersion was further lyophilized and the dry weight was measured. The maximum concentration of the NanoGlue dispersion was 38.5 w/v%.

Adv. Healthcare Mater. **2015**,
DOI: 10.1002/adhm.201500419

Measuring the Force Required to Inject HLAA, NanoGlue, and Cyanoacrylate through 27-Gauge Needles: To measure the injection forces, each 1 mL of HLAA, NanoGlue dispersion in different concentrations (1.8 and 3.7 w/v%), or Dermabond (Ethicon) with or without the activator was loaded within 1 mL plastic syringe (BD) with a 27-gauge 1/2 in. needle (BD). To simulate the forces that would be applied by a surgeon, the syringe barrel was vertically fixed on a mount with the needle facing down and the plunger was pressed downward by a force sensor on a mechanical tester (ADMET) at different injection speeds (0.18, 0.36, 0.72, and 1.44 mL min^{-1}). To test the injection force into aqueous solutions, the needle was submerged in pH 7.4 PBS for 1 min and injected into the PBS. The applied forces were monitored by the software associated with the force sensor. Loading profiles were obtained and the maximum force acquired was quantified. Each experiment was repeated at least three times.

Viscosity Measurement of Native HLAA Glue and NanoGlue Dispersions in Different Concentrations: Viscosities of HLAA and NanoGlue dispersions in different concentrations (0.1–30 w/v%) in water were analyzed using a rheometer (AR-G2, TA Instruments). Dynamic viscosity of each liquid was measured using a 20 mm plate with 200 μm gaps (shear rate: 0.01–100 L s^{-1} in log scale, shear rate of 1 L s^{-1} was selected to compare viscosity of materials).

Measuring the Time to Draw 1 mL of NanoGlue Dispersions through 27-Gauge 1/2 In. Needles: To assess the correlation between NanoGlue dispersion concentration and injectability, the time required to draw 1 mL of NanoGlue dispersions with different concentration (0.1–30 w/v%) using 27-gauge 1/2 in. hypodermic needles were measured. In each experiment, the tip of the needle attached on a 1 mL syringe was dipped into the dispersion vertically and the plunger was quickly pulled up to 1 mL and the time required to draw 1ml was measured manually using an electronic timer.

Visualization of NanoGlue Aggregation upon Exposure to Positive Charged Trigger Using Confocal Microscopy: To visualize the aggregation of NanoGlue particles, low concentration NanoGlue dispersions (3.7 w/v%) was placed onto a glass slide on the fluorescent confocal microscope (Perkin Elmer UltraView RS). Protamine solutions at different concentrations (0.02, 0.1, or 0.5 mg mL^{-1} in water) were added to trigger particle aggregation. Images were acquired every 10 s for 3 min and the size of the particles for each imaging area (0.0145 mm^2) were measured with ImageJ. To filter the background noise from the images, the contrast was adjusted to obtain the sizes of less than 50 particles per imaging area. At least three randomly selected imaging spots were sampled.

Characterization of NanoGlue Morphology Change Before and After the Protamine Treatment Using SEM: To visualize the NanoGlue particles using SEM, the NanoGlue particle dispersion (3.7 w/v% in water) was placed on an oxygen plasma-treated silicon wafer and air-dried. To visualize the reformulated HLAA by treating the NanoGlue particles with protamine, NanoGlue particle dispersion (3.7 w/v% in water) mixed with the same amount of 0.5 w/v% protamine solution in water was placed on an oxygen plasma-treated silicon wafer for 5 min, and further air-dried. The dried samples were sputter-coated with a 10 nm gold film and the particles were visualized via SEM (JEOL 6320 operated at 5 kV).

Mechanical Properties of Reformulated HLAA and Its Cured Product: To assess the mechanical strength of the reformulated HLAA after curing compared to the native HLAA, 30 w/v% NanoGlue dispersion was mixed with 10 mg mL^{-1} protamine solution for 1 min and the precipitated viscous sticky product was carefully collected. The viscous product and the native HLAA were cured with UV light (light intensity: 0.38 W cm^{-2}) for 30 s in 1 mm thick sheets and cut using a dog bone-shaped punch for tensile testing. Each dog bone-shaped sample was immobilized using sample grips at both ends and pulled until break in a rate of 8 mm min^{-1}. The applied force was monitored using a force sensor connected to the mechanical tester. Young's moduli were calculated at 10% strain. Tests were performed in triplicate.

Measurement of the Adhesion Strength of Native HLAA and HLAA NanoGlue Particles: To compare the adhesion properties of the reformulated HLAA and the native HLAA on wet tissue, each glue was placed on a UV-transparent and elastic PGSU patch and cured on heart (epicardium) tissue for pull-off adhesion tests using mechanical tester. Sliced tissue samples were fixed on standard SEM pin stub mount (Ø12.7 × 8 mm pin height, Ted Pella Inc) by instant glue (Loctite 495, Henkel) and wetted with PBS. PGSU films (100–200 μm thick) were prepared according to our published procedure and cut into round patches with the diameter of 6 mm. During the test, SEM pin stubs with tissue samples were loaded on the bottom stage of the mechanical tester (ADMET). Then, 50 μL of 30 w/v% NanoGlue particle dispersion (containing 0.2 w/v% Irgacure 2959 in HLAA, total volume of HLAA: 13 μL) was applied onto the tissue segment, and 50 μL of 10 mg mL protamine solution (500 μg in total) in PBS (pH 7.4) or 50 μL of PBS (pH 7.4) was applied onto the same site. 13 μL of native HLAA was placed on another tissue segment using a positive displacement pipette to compare the adhesion force. After 1 min of glue application, a 200 μm thick PGSU film was placed on top of each glue application site. A UV light guide (Lumen Dynamics Group Inc.) was applied onto the PGSU film with UV transparent borosilicate glass as a nonadhesive spacer to facilitate the release of curing system (i.e., UV light guide and borosilicate glass) without disturbing the patch/adhesive-tissue interface. The glues were cured with UV light (light intensity: 0.38 W cm^{-2}) for 10 s with a compressive force of −3 N. A metal probe with a diameter of 5 mm was attached onto the PGSU patch using instant glue (Loctite 495) and pulled off with a constant strain of 8 mm min^{-1}. The applied force was monitored and the maximum force before full detachment of the patch was measured as the adhesion force. All the experiments were performed in triplicate.

NanoGlue Particle Localization Study in a Mouse Ear with Intravital Confocal Microscopy: BALB/C mice (Charles River Laboratories, Wilmington, MA) were sacrificed immediately before injection and the hair around the base of both ears was trimmed with scissors. Double barrel syringe (Sulzer Mixpac USA, Inc. NH) was adjusted by connecting a 27-gauge needle (BD) to the tip of mixer. Then, 3.7 w/v% NanoGlue particle dispersions were co-delivered with the same amount of either protamine (0.5 mg mL^{-1}) or PBS subcutaneously into the mouse ear with a double barrel syringe. 5 min after the injection, the injection sites were imaged with a custom-built video-rate laser-scanning confocal microscope designed specifically for live animal imaging. To image the surrounding tissue, we positioned the mouse ear on a coverslip (with index matching gels) and obtained high-resolution images with cellular details through the intact mouse skin at depths of up to 250 μm. The laser beams were focused onto the sample (mouse ear skin) using a 60×, 1.2NA water immersion objective lens (Olympus, Center Valley, PA). Fifteen frames were averaged from the live video mode to improve the signal to noise ratio. Excitation of 480 nm was used to induce green autofluorescence of mouse ear skin to indicate the location of the tissue matrix.

Ex Vivo Intraocular Injection of NanoGlue Particles: To visualize the NanoGlue particles, the rhodamine-labeled PGSA was used to fabricate HLAA and NanoGlue particles. The labeled NanoGlue particles showed visible red color under ambient light. High concentration red NanoGlue particle dispersion (30 w/v% in water) was drawn into 1 mL syringe with a 27-gauge 1 in. needle, and the needle was inserted through the anterior part of sclera of a freshly harvested bovine eye (used within 3 d after harvesting). The needle was further maneuvered vertically until it reached the retinal side of the posterior eye, and ≈0.1 mL of the NanoGlue dispersion was injected. The 1ml syringe was then rapidly replaced with another 1 mL syringe containing 10 mg mL^{-1} protamine solution in distilled water or PBS (pH 7.4), and ≈0.05 mL of the protamine solution (or PBS) was injected onto the same site. The eyes were dissected after 5 min of injection and the residual red NanoGlue particles were imaged using a personal use camera (iPhone6, Apple).

Supporting Information

Supporting Information is available from the Wiley Online Library or from the author.

Acknowledgements

Y.L. and C.X. contributed equally to this work. Authors thank Maria J. N. Pereira and Sai Chavala for thoughtful discussions. This work was supported by National Institutes of Health (NIH) grant GM086433 to J.M.K., NIH grant DE013023 to R.S.L., and the Basic Science Research Program through the National Research Foundation of Korea (NRF) funded by the Ministry of Education of Korea (2012R1A6A3A03041166) to Y.L. J.M.K. and R.S.L. hold equity in Gecko Biomedical, a company that has an option to license IP generated by J.M.K. and R.S.L. and that may benefit financially if the IP is licensed and further validated. The interests of J.M.K and R.S.L. were reviewed and are subject to a management plan overseen by their institutions in accordance with their conflict of interest policies.

Received: June 1, 2015
Revised: June 24, 2015
Published online:

[1] W. D. Spotnitz, *Am. Surg.* **2012**, *78*, 1305.
[2] T. O. Smith, D. Sexton, C. Mann, S. Donell, *BMJ* **2010**, *340*, c1199.
[3] B. D. Masini, D. J. Stinner, S. M. Waterman, J. C. Wenke, *J. Surg. Educ.* **2011**, *68*, 101.
[4] P. Andrades, A. Prado, S. Danilla, C. Guerra, S. Benitez, S. Sepulveda, C. Sciarraffia, V. De Carolis, *Plast. Reconstr. Surg.* **2007**, *120*, 935.
[5] M. Petri, M. Ettinger, A. Dratzidis, E. Liodakis, S. Brand, U. V. Albrecht, C. Hurschler, C. Krettek, M. Jagodzinski, *Arch. Orthop. Trauma Surg.* **2012**, *132*, 649.
[6] L. Johnson, T. E. Cusick, S. D. Helmer, J. S. Osland, *Am. J. Surg.* **2005**, *189*, 319.
[7] B. Suc, S. Msika, A. Fingerhut, G. Fourtanier, J.-M. Hay, F. Holmières, B. Sastre, P.-L. Fagniez, *Ann. Surg.* **2003**, *237*, 57.
[8] T. Landegren, M. Risling, J. K. E. Persson, A. Sondén, *Int. J. Oral Maxillofac. Surg.* **2010**, *39*, 705.
[9] Y. C. Tseng, Y. Tabata, S. H. Hyon, Y. Ikada, *J. Biomed. Mater. Res.* **1990**, *24*, 1355.
[10] B. J. Vote, M. J. Elder, *Clin. Exp. Ophthalmol.* **2000**, *28*, 437.
[11] P. Klimo, A. Khalil, J. R. Slotkin, E. R. Smith, R. M. Scott, L. C. Goumnerova, *Neurosurgery* **2007**, *60*, 305.
[12] N. Lang, M. J. Pereira, Y. Lee, I. Friehs, N. V. Vasilyev, E. N. Feins, K. Ablasser, E. D. O'Cearbhaill, C. Xu, A. Fabozzo, R. Padera, S. Wasserman, F. Freudenthal, L. S. Ferreira, R. Langer, J. M. Karp, P. J. del Nido, *Sci. Transl. Med.* **2014**, *6*, 218ra6.
[13] J. C. Rosser, L. E. Rosser, R. S. Savalgi, *Arch. Surg.* **1997**, *132*, 200.
[14] T. Sato, K. Yamazaki, *Clin. Exp. Gastroenterol.* **2010**, *3*, 91.
[15] O. B. Rickman, J. P. Utz, G. L. Aughenbaugh, C. J. Gostout, *Mayo Clin. Proc.* **2004**, *79*, 1455.
[16] B. D. Hemond, A. Taberner, C. Hogan, B. Crane, I. W. Hunter, *J. Med. Devices* **2011**, *5*, 015001.
[17] J. C. Stachowiak, T. H. Li, A. Arora, S. Mitragotri, D. A. Fletcher, *J. Controlled Release* **2009**, *135*, 104.
[18] L. McAllister, J. Anderson, K. Werth, I. Cho, K. Copeland, N. Le Cam Bouveret, D. Plant, P. M. Mendelman, D. K. Cobb, *Lancet* **2014**, *384*, 674.
[19] S. Mitragotri, *Nat. Rev. Drug Discovery* **2006**, *5*, 543.
[20] H. G. Silverman, F. F. Roberto, *Mar. Biotechnol.* **2007**, *9*, 661.
[21] H. Lee, N. F. Scherer, P. B. Messersmith, *Proc. Natl. Acad. Sci. U.S.A.* **2006**, *103*, 12999.
[22] J. H. Waite, N. H. Andersen, S. Jewhurst, C. Sun, *J. Adhes.* **2005**, *81*, 297.
[23] J. Yu, W. Wei, E. Danner, R. K. Ashley, J. N. Israelachvili, J. H. Waite, *Nat. Chem. Biol.* **2011**, *7*, 588.
[24] L. Khandeparker, A. C. Anil, *Int. J. Adhes. Adhes.* **2007**, *27*, 165.
[25] D. E. Barlow, G. H. Dickinson, B. Orihuela, J. L. Kulp, D. Rittschof, K. J. Wahl, *Langmuir* **2010**, *26*, 6549.
[26] N. V. Gohad, N. Aldred, C. M. Hartshorn, Y. J. Lee, M. T. Cicerone, B. Orihuela, A. S. Clare, D. Rittschof, A. S. Mount, *Nat. Commun.* **2014**, *5*, 4414.
[27] M. Wiegemann, T. Kowalik, A. Hartwig, *Mar. Biol.* **2006**, *149*, 241.
[28] C. S. Wang, R. J. Stewart, *J. Exp. Biol.* **2012**, *215*, 351.
[29] C. S. Wang, R. J. Stewart, *Biomacromolecules* **2013**, *14*, 1607.
[30] C. Wang, K. Svendsen, R. Stewart, *Biological Adhesives Systems Adhesives Systems* (Ed: I. Grunwald), University of Vienna, Springer **2010**, 169.
[31] H. Shao, K. N. Bachus, R. J. Stewart, *Macromol. Biosci.* **2009**, *9*, 464.
[32] A. Lorenz, N. Städtler, H. J. Schulz, *Endoscopy* **2002**, *34*, 670.
[33] A. Inaganti, S. Duvuru, S. Komanapalli, N. S. Samji, P. Roy, *Am. J. Gastroenterol.* **2012**, *107*, S751.
[34] T. Chen, R. Janjua, M. K. McDermott, S. L. Bernstein, S. M. Steidl, G. F. Payne, *J. Biomed. Mater. Res. Part B Appl. Biomater.* **2006**, *77*, 416.
[35] M. J. Taravella, C. D. Chang, *Cornea* **2001**, *20*, 220.
[36] Y. M. Bhat, S. Banerjee, B. A. Barth, S. S. Chauhan, K. T. Gottlieb, V. Konda, J. T. Maple, F. M. Murad, P. R. Pfau, D. K. Pleskow, U. D. Siddiqui, J. L. Tokar, A. Wang, S. A. Rodriguez, *Gastrointest. Endosc.* **2013**, *78*, 209.
[37] D. B. Genovese, *Adv. Colloid Interface Sci.* **2012**, *171*, 1.
[38] V. Y. Rudyak, *Adv. Nanopart.* **2013**, *2*, 266.
[39] E. Sekiyama, T. Nakamura, E. Kurihara, L. J. Cooper, N. J. Fullwood, M. Takaoka, J. Hamuro, S. Kinoshita, *Investig. Ophthalmol. Vis. Sci.* **2007**, *48*, 1528.
[40] M. Takaoka, T. Nakamura, H. Sugai, A. J. Bentley, N. Nakajima, N. J. Fullwood, N. Yokoi, S. H. Hyon, S. Kinoshita, *Biomaterials* **2008**, *29*, 2923.
[41] P.-A. Mackrodt, *J. Fluid Mech.* **1976**, *73*, 153.
[42] B. Güzel, T. Burghelea, I. A. Friggard, D. M. Martinez, *J. Fluid Mech.* **2009**, *627*, 97.
[43] B. Eckhardt, T. M. Schneider, B. Hof, J. Westerweel, *Annu. Rev. Fluid Mech.* **2007**, *39*, 447.
[44] S. J. Shire, Z. Shahrokh, J. Liu, *J. Pharm. Sci.* **2004**, *93*, 1390.
[45] J. Liu, M. D. H. Nguyen, J. D. Andya, S. J. Shire, *J. Pharm. Sci.* **2005**, *94*, 1928.